# Molecular dynamics studies on the effect of surface roughness and surface tension on the thermodynamics and dynamics of hydronium ion transfer across the liquid/liquid interface

Ilan Benjamin*

*Department of Chemistry and Biochemistry,*

*University of California, Santa Cruz, California 95064, USA*

## ABSTRACT

Molecular dynamics simulations are used to examine the effect of surface roughness and surface tension on the transfer of the classical hydronium ion ($H_3O^+$) across the water/1,2-dichloroethane interface. Free energy of transfer, hydration structure and dynamics as a function of the ion location along the interface normal are calculated with 6 different values of a control parameter whose variation modifies the surface tension without impacting the bulk properties of the two solvents. Transfer of the classical hydronium ion across the water/1,2-dichloroethan interface involves the co-transfer of three hydration shell water molecules independent of the surface tension. However, as the interaction between the two liquids weakens, rise in interfacial tension and decrease in intrinsic water fingering and capillary fluctuations results in fewer water molecules co-transported with the ion in the second shell and a reduction in the length of the finger that the ion is attached to, consistent with the reduced size of the second hydration shell. First shell water residence time and lateral ion diffusion constants varies with the surface tension in a way that are consistent with the above structural insight.

---

* Email address: ilan@ucsc.edu

## I. INTRODUCTION

It is well-known that the presence of ions at water/nonpolar liquid interfaces generally increases the interfacial tension and consequently decreases the interfacial width, while the adsorption of surfactants has the opposite effect[1]. Capillary wave theory associates the change in interface width with the change in the amplitude of capillary waves[2]. This average thermodynamic view is not quite useful for understanding the mechanism of processes such as ion transfer (both electrochemical and assisted transfer) and ion extraction at the liquid/liquid interface. Thus, molecular dynamics simulations where the microscopic structure of the interface is examined during these processes are highly beneficial for gaining mechanistic insight and for understanding how surface roughness influences ion distribution and transfer beyond examination of average properties[3-11]. These simulations as well as some analytical theories[12-14] suggest that the process of ion adsorption and transfer across the interface between water and an immiscible organic solvent is strongly coupled to water finger-like structures.

One way to quantify the local structure and its correlation with ion's adsorption and transfer is through the concept of the instantaneous surface[15-18]. By identifying the true interfacial region vs. the bulk-like region, ion distribution at the interface can be understood[11]. Another approach is to describe the ion transfer process using generalized coordinates, which take into account surface roughness and the local thermodynamic state of the ion[7, 9, 19]. In both of these approaches one typically controls the ion location and/or the ion density and study the resulting effect on the interface structure and the feedback effect on the ion distribution.

A complimentary approach to the above studies that has not been extensively considered and could further shed light on the microscopic manifestation of the effect of surface tension is the examination of the effect of varying the surface tension of the interface on ion transfer thermodynamics and dynamic. This can be done by an applied electric field[20, 21] or added surfactants as mentioned above, but these studies can directly impact the ion transfer process by changing the intrinsic free energy of transfer. In this work we consider an approach that will allow for disentangling the contribution of the interfacial surface tension in order to gain new insight on the effect of a change in the interface structure on the ion transfer process. In this respect our work is the microscopic analogue of the continuum model approach of Verdes *et al.* [14] based on the Kornyshev–Kuznetsov–Urbakh 2D coupled non-linear Lengevin equation[22]. In that work it was shown that in general,due to the effect of surface protrusions, an increase in surface tension results in lower ion transfer rate.

Our methodology for controlling the surface tension without changing the thermodynamic properties of the two bulk liquids has been used in our previous work on the effect of surface tension on the rotational correlation time of a molecular solute adsorbed at the interface[23]. By controlling the strength of the Lennard-Jones interaction between molecules of the two immiscible liquids, one can change the surface tension and other surface structural properties without changing the bulk properties of the two liquids.

The choice of studying the transfer of the hydronium ion in this work is motivated by recent work suggesting the possible role of proton transfer reactions in facilitating the complexation of the extractant molecules with the hydrated ion. This proton transfer reaction may be driven by an access proton adsorption at the interface[24]. Another motivation for examining classical proton transfer across the interface in this work, is to setup a benchmark for future work when the quantum mechanical nature of the proton is examined.

The rest of this paper is organized as follows. In section II we describe the systems, potential energy functions and other simulation details. In section III we discuss the results of these calculations and in section IV we summarize this work and present our conclusions.

## II. SYSTEMS AND METHODS

### A. System description and potential energy functions

The systems studied include a single hydronium ion located in different locations of water/DCE interface formed by two adjacent slabs of 500 water molecules and 214 1,2-dichloroethane (DCE) molecules in a 24.8 × 24.8 × 100.0 Å rectangular box. Each liquid phase is in equilibrium with its respective vapor phase so only one liquid/liquid interface is present, located in the $X$-$Y$ plane at $Z \approx 0$. The water phase in the region of $Z < 0$ and the DCE phase in the $Z > 0$ region. Periodic boundary conditions are applied in all directions and a reflecting wall is located 5 Å from the simulation box boundaries in the $Z$-direction to prevent mixing of the two vapor phases.

The potential energy functions used in this work have been extensively used in our previous work. They have been shown to give good agreement with experimental hydration free energy and surface tension. For water, a flexible version of the SPC model with intramolecular potentials of Kuchitsu and Morino[25] are used. The DCE molecules are modeled using a 4-site flexible model previously described[26] that reproduces the experimental dipole moment and enthalpy of vaporization of DCE. The intermolecular interaction potentials are represented as the pairwise sum of Lennard-Jones (LJ) and Coulomb terms:

$$u_{ij}(r) = 4\varepsilon_{ij}\left[\left(\sigma_{ij}/r\right)^{12} - \left(\sigma_{ij}/r\right)^{6}\right] + \frac{q_i q_j}{4\pi\epsilon_0 r} \quad , \qquad (1)$$

where $r$ is the distance between atom centers $i$ and $j$. Standard Lorentz-Berthelot combining rules, $s_{ij} = (s_i + s_j)/2$ and $\varepsilon_{ij} = (\varepsilon_i \varepsilon_j)^{1/2}$ are used to generate LJ parameters for the mixed interactions between water-water and DCE-DCE molecules. The LJ intermolecular interactions between water -DCE molecules are scaled by a factor $f_S$:

$$\varepsilon_{ij} = f_S (\varepsilon_i \varepsilon_j)^{1/2}, \tag{2}$$

where the index $i$ refers to the O or H atoms of water and the index $j$ for Cl or C atoms of DCE. As shown in detail below, this factor enables us to control the surface tension at the water/DCE interface. When $f_S = 1$, the experimental surface tension of water/DCE is reproduced. In the simulations described below we select the values $f_S = 0.1, 0.3, 0.5, 0.7, 0.9$ in addition to $f_S = 1.0$.

For the interactions between the hydronium ion and the two liquids, we use in this work a classical force field. Cleary a fully classical description has significant limitations in accounting for all the observed structural, thermodynamic and kinetic properties of the excess proton[27]. Nevertheless, classical models can provide important insight when they are compared with models that incorporate some quantum aspects of the proton and contrasted with experiments[28]. Several classical force fields for interaction between the hydronium ion and water and other molecules have been discussed in the literature[28-31]. Our choice is based on the SPCE model of Wolf and Groenhof[30]. They have examined several classical models as well as an approach to account for the proton's quantum dynamics and found the difference between them to be small. Our implementation here is fully classical. We recently used this model to calculate the free energy of transfer of $H_3O^+$ from water to DCE with reasonable agreement with experimental data[10].

## B. Methods

To examine the thermodynamics, structural and dynamic properties of the hydronium ion as a function of the distance along the interface normal we place the $H_3O^+$ cation in $N$ overlapping lamellas, each 2Å-wide, spanning the region from bulk water to bulk DCE. In each lamella, a 4 ns constant temperature (T = 298K) Molecular Dynamics (MD) trajectory is performed. The ion is constrained within a specified lamella by a window potential, which is zero when the ion is inside that window but rises rapidly when the ion is outside the window. This allows for statistically accurate calculations of several structural and dynamical properties of the cation as a function of the distance from the interface. The free energy profile for the transfer of the cation across the interface is determine using the umbrella sampling method[32]. First, the probability distribution of the ion position $z_I$ in each lamella is used to calculate the corresponding free energy $A_n(Z)$

$$A_n(Z) = -k_B T ln P_n(Z), \quad P_n(Z) = \langle \delta(Z - z_I) \rangle \quad , \tag{3}$$

where $\delta$ is the Dirac delta function and $P_n(Z)$ ($n$ = 1,2,…$N$) is the ion $Z$ coordinate probability distribution within lamella $n$ and the ensemble average (denoted by the triangular brackets) is calculated over all possible solvent configurations while the ion is located at $z_I = Z$. Next, the series of $A_n(Z)$ segments is combined by using their overlapping region[33, 34]. All the MD simulations are performed with our in-house software that uses the velocity Verlet algorithm with an integration time-step of 0.5 fs.

The free energy, structural and dynamical calculations as a function of the ion location across the interface are carried out for 5 different systems corresponding to 5 different values of the water/DCE surface tension by selecting the values of the coupling parameter *f*s to be 0.1, 0.3, 0.5, 0.7, 0.9, in addition to the results with *f*s = 1.0 previously published. Note that values of *f*s >1 produce partial miscibility of the two liquids and an unstable liquid/liquid interface.

## II. RESULTS AND DISCUSSION

### A. The neat interface

The properties of the neat water/DCE interface have been described in detail elsewhere.[26] Here we focus on the impact of varying the coupling constant *f*s on some aspects relevant to the excess proton in the system.

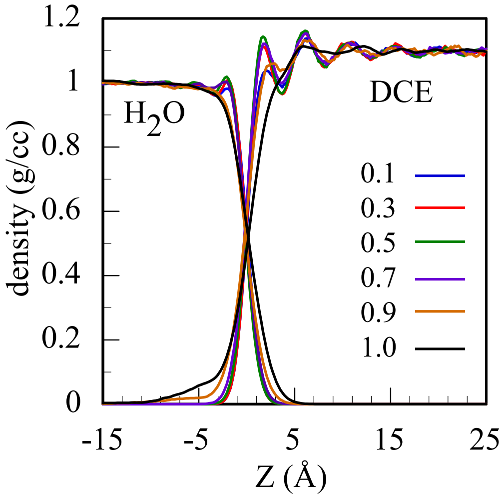

**FIG. 1**. Density profiles of water and 1,2-dichloroethane at T = 298K for the different choice of the coupling constant *f*s (values listed in the legend).

The density profiles of water and DCE in the neat system (no ion) are shown in Fig. 1 for the different value of the coupling parameter *f*s. As the strength of the interaction between the water and DCE molecules decreases (*f*s decreases from 1 to 0.1), the interface sharpens and oscillations in the densities are observed as a result of the molecular staking against the effective hard wall presented to each liquid by the molecules of the second liquid. The change in width can be quantified by fitting the tail of the water density profile $\rho(z)$ to the following expression (obtained from the van der Waals mean field approximation [2]):

$$\rho(z) = \frac{1}{2}\rho_{BW}\left[1 - \tanh\left(\frac{z-z_G}{2\delta}\right)\right] \tag{3}$$

where $\rho_{BW}$ is the water's bulk density, $z_G$ is the position of the Gibbs Dividing Surface (the plane parallel to interface where the water density is approximately half the bulk value. For the exact definition see [2]), and $\delta$ is a measure of the interface width. The width is typically expressed as the distance over which the density changes from 90% to 10% of the bulk density. This is equal to $4.4\delta$ if the mean field expression for $\rho$ (Eq. 3) is used. This width is also directly related to the surface tension $\gamma$ of the system. Specifically, capillary wave theory confirmed by simulations[8] shows that $\delta \propto \sqrt{T/\gamma}$.

Fig. 2 shows marked decrease in the width as $f_S$ decreases from 1 to 0.1, plateauing when $f_S$ is around 0.5. The figure also shows the total water-DCE intermolecular interaction energy, $U_{WD}$, which varies from −200 kcal/mol to −30 kcal/mol as $f_S$ decreases from 1 to 0.1. The variation in $U_{WD}$, is more dramatic then the change in the interface width and unlike the width it does not reach a plateau. This is because two factors contribute to the value of $U_{WD}$: 1) The direct reduction in the pair interaction energy due to the reduced value of $f_S$, and 2) the reduced width results in diminished probability to find close water-DCE neighbors.

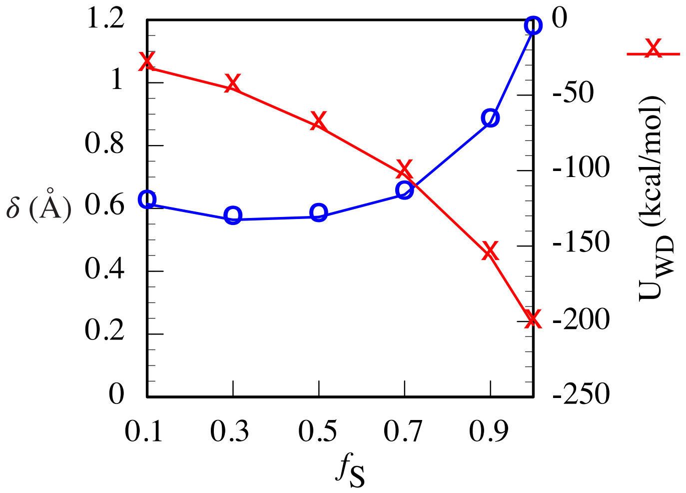

**FIG. 2**. The interfacial width parameter δ (see Eq. 3, circles connected by a blue line), and the total water/DCE interaction energy (X connected by a red line) vs. the coupling constant $f_S$ .

While the interfacial width and the water/DCE interaction energy are useful characterization of how the neat interface structure varies with the coupling parameter, it is important to note that when the ion is at the interface, significant perturbation of this structure is observed and must be taken into account for understanding the behavior of the ion, as will be discussed below.

### B. Structural and thermodynamic properties of the hydronium at the interface

The free energy profiles for the transfer of the hydronium ion across the different water/DCE interfaces are shown in Figure 3. The free energy curves monotonically increase as the ion is transferred across the interface from bulk water to bulk DCE. As the coupling constant $f_S$ decrease from 1 toward 0.1 (resulting in a narrower interface region), the free energy profiles get narrower, but are still broader than the respective width of the water density profile (Figure 1). Interestingly, the net free energy of transfer moderately increases as the surface tension increases. This may seem surprising since the interaction of the hydronium ion with the two bulk liquids is independent of the interaction between the two liquids.

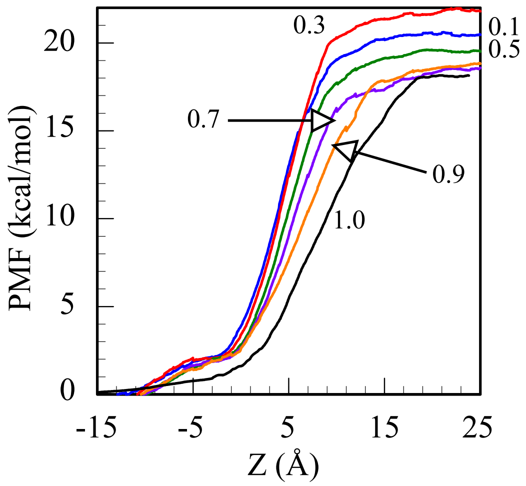

**FIG. 3.** The free energy profile for the transfer of $H_3O^+$ across the water/DCE interface for the different choice of the coupling constant *f*s (values listed in the plot).

To understand the impact of the interface surface tension (as determined by the coupling constant *f*s) on the free energy of transfer, it is important to realize that the ion transfer is facilitated by the ability of the ion to hold onto some of the water molecules. This has been demonstrated by numerous molecular dynamics studies looking at different ions across different interfaces[7, 9, 35-38]. We demonstrate this water "dragging" effect by computing as a function of the ion's location the average number of water molecules in its first and second hydration shells as the ion is transferred across the interface.

The average number of water molecules in the first hydration shell $N_1^{sh}$ is defined by:

$$N_1^{sh}(r) = \int_0^{R_{min}^{(1)}} 4\pi\rho_W\, g(r) r^2 dr \,, \tag{4}$$

where $\rho W$ is the bulk water density (0.0334 $Å^{-3}$), $g(r)$ is the ion-water oxygen radial distribution function and $R_{\min}^{(1)}$= 2.9Å is the first minimum of $g(r)$ (and is independent of the particular water/DCE system). In practice we compute this number by counting the number of water molecules whose oxygen-ion distance is less than $R_{\min}^{(1)}$ at each time step and average over all time steps. The average number of water molecules in the second hydration shell $N_2^{sh}$ is defined by:

$$N_2^{sh}(r) = \int_{R_{min}^{(1)}}^{R_{min}^{(2)}} 4\pi\rho_W\, g(r) r^2 dr \,, \tag{5}$$

where $R_{\min}^{(2)}$ is the location of the second minimum of $g(r)$. This value slightly changes from system to system.

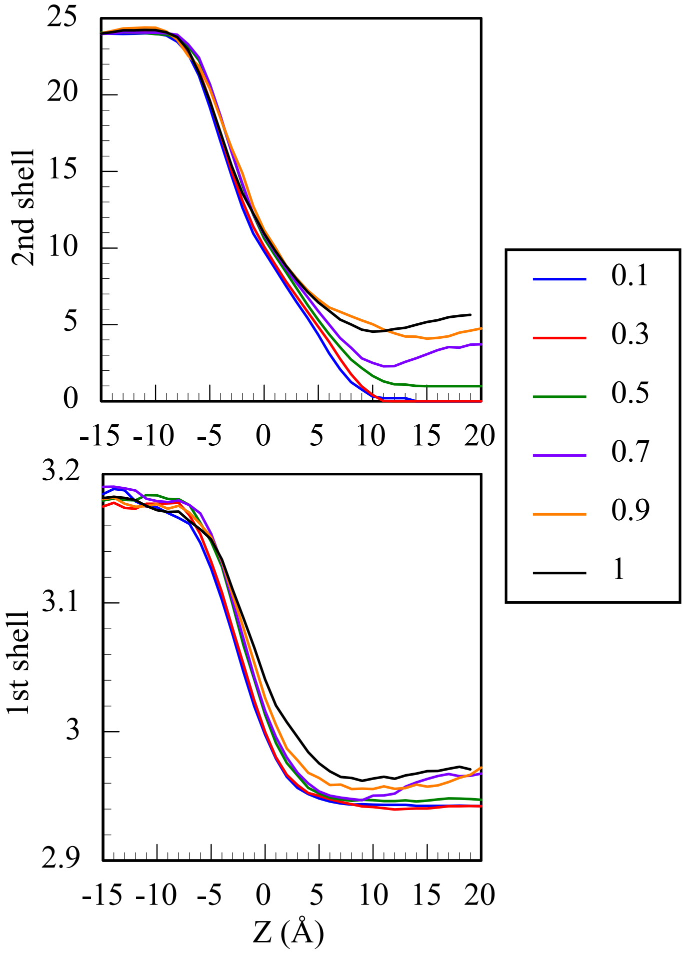

**FIG. 4**. The number of water molecules in the 1st (bottom panel) and 2nd (top panel) hydration shell of the hydronium ion as a function of its distance along the interface normal ($Z = 0$ is the location of the Gibbs Dividing Surface) for the different choice of the coupling constant *f*s (values listed in the legend).

The results are shown in Figure 4. The first hydration shell number varies from 3.18 when the ion is in bulk water to near 3 as the ion is transferred to DCE, almost independent of the system. This means that the hydronium ion is essentially transferred as a conserved Eigen-like species $H_9O_4^+$. Note that since our treatment is fully classical, the "Eigen-like" species refers to a classical hydronium cation symmetrically solvated by three water molecules, and not the quantum mechanical object, which is a distorted structure where the net +1 charge is dynamically delocalized across the four oxygen atoms[57]. In bulk water there is an additional water molecule hovering around the cation that is rarely able to get close enough to count as part of the first hydration shell slow exchange process (see below). In bulk DCE one of the three water molecules that make up the Eigen complex can get farther away during the exchange process and not counted, which leads to $N_1^{sh}$ being slightly less than 3.

More interesting are the results for the second hydration shell. $N_2^{sh}$ is about 24 in bulk water (obviously independent of the particular water/DCE system). It markedly drops as the ion cross the interface. The final value of $N_2^{sh}$ (when the ion is in bulk DCE) varies from about $N_2^{sh}$= 5 when *f*s = 1 to $N_2^{sh}$= 0 when *f*s < 0.5. Clearly, the number of water molecules that are dragged with the Eigen complex decreases as the surface tension increases.

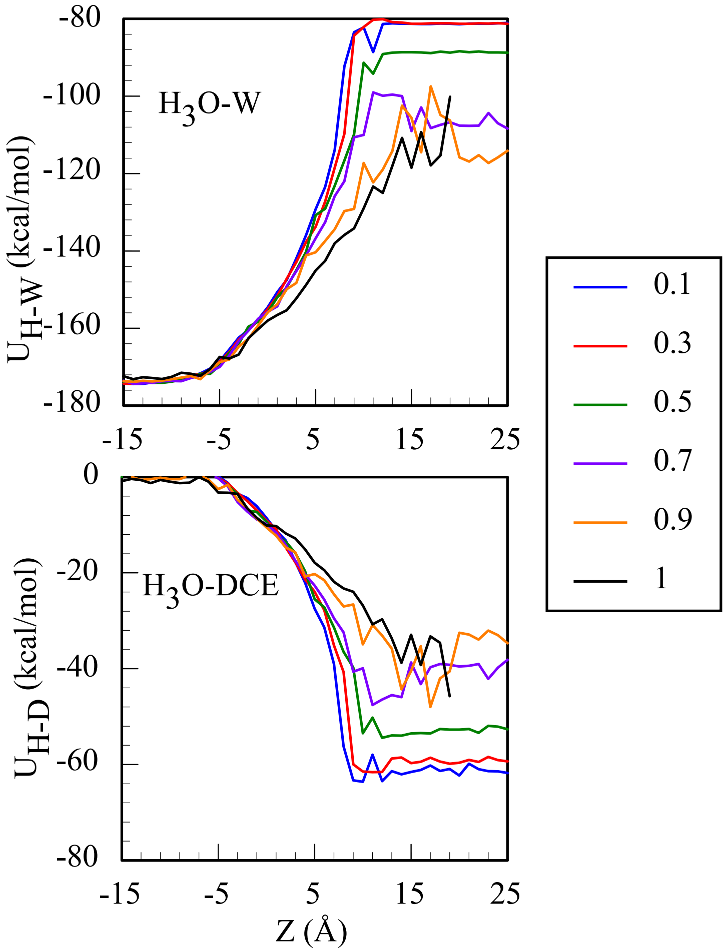

**FIG. 5**. Total $H_3O$-Water (top panel) and $H_3O$-DCE (bottom panel) interaction energy for the different choice of the coupling constant $f_S$ (values listed in the legend).

As another demonstration of the influence of the surface roughness (and by direct association the surface tension) on the degree of water molecules co-transfer with the ion, Figure 5 shows the total ion-water and ion-DCE interaction energies. As the surface tension increases and the intrinsic water fingering and capillary fluctuations decreases, fewer water molecules are transported with the ion in the second shell, which result in weaker water-ion interactions, but more ion-DCE interactions (since the ion is more exposed to interactions with the organic solvent).

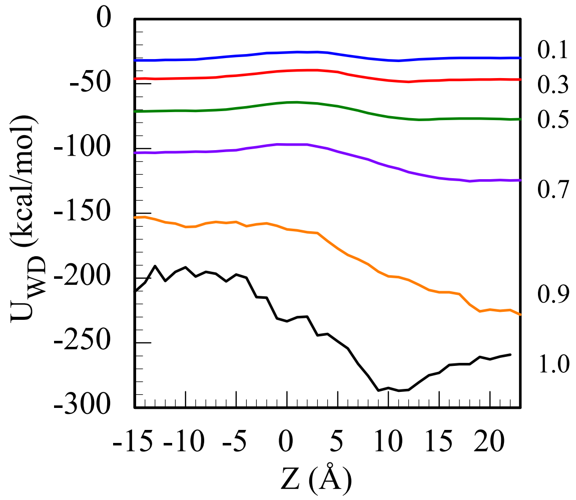

**FIG. 6**. Total DCE-Water interaction energy as a function of the location of the hydronium ion along the interface normal ($Z = 0$ is the location of the Gibbs Dividing Surface) for the different choice of the coupling constant $f_S$ (values listed on the right).

The degree of intermixing of the two liquids, which diminishes as $f_S$ decreases has already been pointed out for the neat interface in Figure 2. Figure 6 shows this quantity for each system (each value of $f_S$) as the ion is transported across the interface. This figure can also be used to monitor the degree of increased surface roughness due to the ion crossing the interface. For small values of $f_S$, the water-DCE interaction energy ($U_{WD}$) remains nearly flat as the ion crosses the interface. The slight drop is due to essentially the additional water/DCE contact produced by the Eigen complex. As $f_S$ increases to 0.7 and to 0.9, the increased (negative) interaction energy correspond to the significantly more water-DCE contacts produced when part of the second hydration shell co transferred with the ion to DCE. Note that when $f_S = 1$, the significant perturbation to the interface and the marked mixing results in large negative change to $U_{WD}$ as the ion crosses the interface, but spring back up when these water fingers return to their neat interface length.

The significant perturbation of the structure of the neat interface and the formation of water protrusions in the form of a single file water molecules (“fingers”) have been discussed in details elsewhere[7, 9, 10]. Here we briefly describe how the length of these water “fingers” depends on the surface tension of the neat interface.

Figure 7 depicts an example of a chain of water molecules connecting the hydrated hydronium ion that is deep in the DCE phase to the aqueous phase.

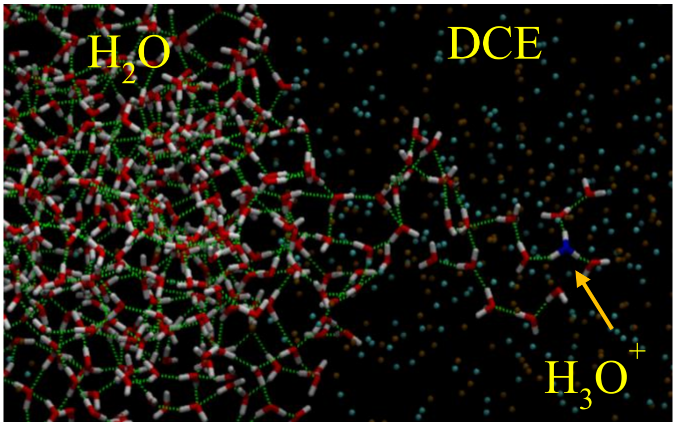

**FIG. 7.** A hydronium ion (blue oxygen) in the DCE phase connected via a water “finger” to the aqueous phase. The hydrogen bonding network is shown in green dotted lines

To quantify the length of these water protrusion we can use the procedure suggested by Kikkawa *et. al.* [7]. The ion and water molecules are treated as vertices in an undirected graph whose edges are the geometrical distances between the vertices. A connected path between the ion and bulk water is defined by the requirement that all edges along the path are shorter than a threshold distance. The coordinate $w$ is defined to be equal to the minimum threshold distance that will give rise to a connected path. More details about our specific implementations can be found in[9, 10].

When the ion is in bulk water $\langle w \rangle$ ≈ peak position of the water O-O Radial Distribution Function of SPCE water[39] = 2.75Å. When the ion is in the organic phase connected by a water "finger" to the aqueous phase, $w$ ≈ O-O distance corresponding to the longest hydrogen bond, around 3.4Å (corresponding to the location of the first minimum of the OO radial distribution function in bulk water). As the water "finger" breaks, $w$ corresponds to the distance between the two nearest water molecules – one that belong to the ion hydration shell and one to the water phase.

Water finger breakup dynamics and energetics have been described in details elsewhere for the case of $f_S = 1$[10]. Briefly, as the ion is constraint to windows that are located deeper in the organic phase (larger $Z$ values) the probability of finger breakup increases. Finger breakup can be followed by an increase in the value of $w$ to a value as big as 14Å and yet followed by finger reformation ($w$ returns to values less than 3.4Å), immediately or after a significant time delay. Eventually, at some large enough value of Z, finger reformation is no longer observed (on the 4 ns time scale) and the water finger retracts to the aqueous phase. Examination of individual trajectories suggests that $w(t)$ close to breakup point experience significant re-crossing dynamics where $w$ fluctuates around some distance around 3.4 Å before finally a breakup is observed. To avoid counting these fluctuations as "real" breakup events we chose a critical "transition state" distance $w_c$ = 6Å so that a water finger breakup is defined when $w > w_c$. (This distance is approximately when the free energy associated with extending the finger reaches a plateau[10]. ) Denoting by $P_n$ the probability that the water finger is broken ($w > w_c$) while the ion is in window $n$ and by $Z_n$ the average value of the ion position when $0 < w - w_c < 0.5$Å (this gives an estimate of the breakup point to within 0.5Å), the average location of the ion relative to the Gibbs surface when the water finger is broken is then simply $\langle Z_b \rangle = \sum_n P_n Z_n$. The value

$\sim\langle Z_b\rangle - w_c$ is an estimate of the average water finger length at breakup. The standard deviation in the distribution of $Z_n$ values is given by $\sigma_b = \sqrt{\langle Z_b^2\rangle - \langle Z_b\rangle^2}$.

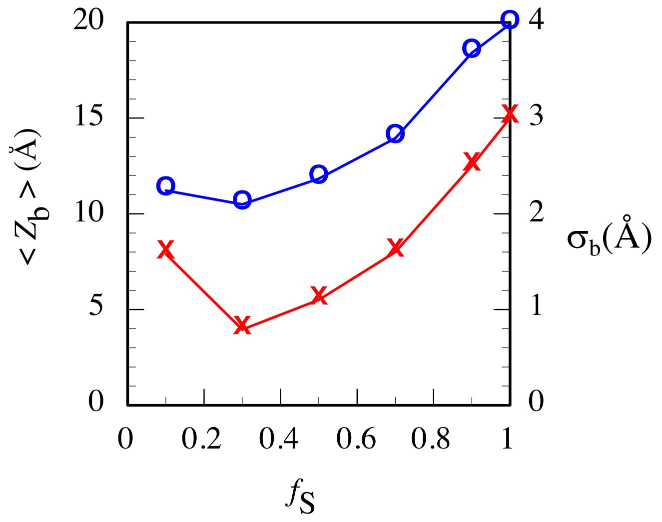

**FIG. 8.** Average location (blue open circles) relative to the GDS and the standard deviation from the average, (red X) of the hydronium ion when the water "finger" connecting it to the bulk water phase breaks vs. the coupling parameter *f*S.

Figure 8 shows that except for the lowest value of the coupling constant *f*S, reducing *f*S, (reducing the roughness and the amplitude of the intrinsic water fingers in the neat interface) leads to a reduction in the length of the finger that the ion is attached to. This is consistent with the reduced size of the second hydration shell and provide further evidence that the magnitude of the fingering and roughness of the neat interface carries over to the ion transfer process, which is facilitated by the formation of water finger-like structure.

## C. Dynamical properties

Additional information about surface tension effects on ion transfer can be gained by examination of several dynamical properties characterizing the state of the ion in lamellas parallel to the interface as a function of its position along the interface normal. While the ion is held in the 2Å-wide lamella, the 4 ns MD equilibrium trajectory is sufficiently long to obtain these results.

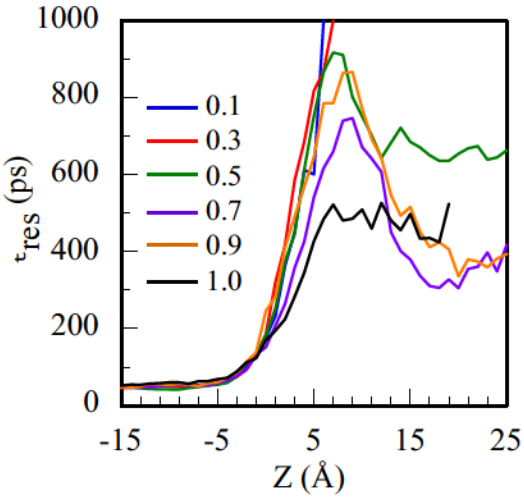

**FIG. 9.** Average residence time of water molecules in the first hydration shell of a hydronium ion vs. the location of the ion along the interface normal for the different choice of the coupling constant $f_S$.

As shown above, regardless of the water/DCE interaction parameter defining the system under study, the hydronium ion remains coordinated to 3 water molecules as it moves in the aqueous phase and across the interface into the DCE phase. However, these water molecules are not permanently attached to the ion and they could be exchanged with nearby water molecules. The dynamics of water molecules exchanging between the first and second shell have been examined extensively for ions of different charge and size in bulk water[40-42], at liquid interfaces [4] and in hydrophobic media.[43, 44] The residence time of water molecules in the hydronium ion's first hydration shell is determined by following the residence time correlation function:[40, 41, 45-47]

$$C_{\text{res}}(t) = \frac{1}{n(t)} \sum_{i=1}^{N} \langle h_i(t+t')h_i(t') \rangle \,, \tag{6}$$

where for each water molecule "*i*", $h_i(t) = 1$ as long as this water molecule is inside the first hydration shell (or leave for a time period shorter than some lag time, which we take to be 2 ps). $N$ is the total number of water molecules, $n(t)$ is the number of water molecules in the first hydration shell at time $t$ and the ensemble average is taken over all the time origins $t'$. The average residence time is then obtained from the time integral of $C_{\text{res}}(t)$.

The calculated residence time of water molecules in the first hydration shell of $H_3O^+$ in bulk water is around 70 ps, independent of course of the system and is similar to the one obtained by Roy and Dang using a polarizable hydronium potential.[48] Figure 9 shows that the residence time rises sharply as the hydronium ion reach the Gibbs surface independent of the system, but than diverges depending on $f_S$ as the ion crosses the interface.

When $f_S$ is small (less than 0.5) and Z > 5Å, not much water is dragged with the ion and the residence time is too long to accurately determine in our simulations, the ion simply hold into the set of water molecules that is in the first shell at this point. For higher values of $f_S$ the calculated residence time is still significantly larger than in bulk water. This is due to the fact that for a water molecule to exit the tightly bound first hydration shell, a different water molecule has to enter the hydration shell before or very shortly after. The availability of such water molecules is greatly reduced when the second hydration shell is beginning to be depleted as the ion cross the interface. Note that when the ion is connected to the bulk aqueous phase by a narrow water finger, the residence time is longer than after the “finger” is broken, which explains the initial rise and drop in the residence time. The increase in the residence time as the ion crosses the interface has been observed for other ion transfer cases across liquid/liquid interfaces[4] and around hydrated ions in hydrophobic media[43, 44].

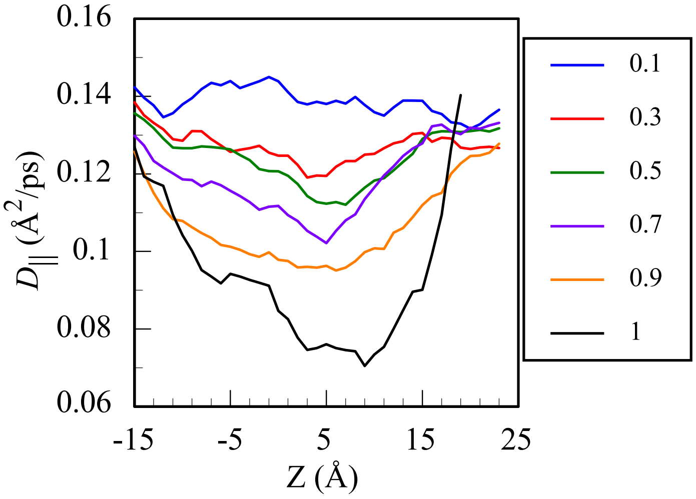

**FIG. 10.** Lateral diffusion coefficient of the ion restricted to 2Å windows parallel to the interface vs. the location of the ion in the window for the different choice of the coupling constant $f$s.

Another measure of ion dynamics that can be influenced by the liquid/liquid interface roughness is the ion’s diffusion constant. While the diffusion constant can be easily determined in bulk liquids from conductivity measurements, complications arise at interfaces due to the fact that the ion motion is not isotropic: translation parallel and perpendicular to the interface are different and depends on the ion location along the interface normal. Also, diffusion perpendicular to the interface cannot be distinguished from the ion transfer process itself. Molecular dynamics simulations are thus an important tool for elucidating ion diffusion at the interface. Whereas in bulk liquid the isotropic diffusion constant $D$ can be calculated from the mean square displacement (MSD) time correlation function using the relation:[49] $\lim_{t\to\infty}\langle[\mathbf{r}(t)-\mathbf{r}(0)]^2\rangle = 6Dt,$ at an interface, a different procedure is necessary for determining the ion's $Z$-dependent diffusion coefficients in the direction normal, $D_{ZZ}(z)$, and parallel, $D_{xx}(z) = D_{yy}(z) = D_{||}$, to the interface.

Our simulation methodology, whereby the ion is restricted to a set of narrow lamellas parallel to the interface allows us to easily determine $D_{||}$ from the MSD calculated from the long simulation trajectory in each lamella:

$$\lim_{t\to\infty}\langle[\mathbf{s}(t)-\mathbf{s}(0)]^2\rangle = 4D_{||}(z)t \qquad , \tag{7}$$

where $\mathbf{s} = (x, y)$ is the projection of the vector position of the ion onto the plane parallel to the interface. Note that since the distance travelled by the ion in the narrow lamella is relatively short (3Å or less), $D_{ZZ}$ cannot be reliably computed from the limiting value of the MSD in the $Z$ direction. A fit of the MSD to a diffusion equation have been used to compute this value.[50, 51] Here this quantity is not quite useful since the dynamic along $Z$ is intimately connected with the interface crossing and the rate determining step is overcoming the free energy barrier for the ion transfer.

Before describing the interfacial results, it is useful to briefly review ion mobility in bulk solution in general and that of the hydronium ion in particular. Diffusion of small neutral molecules in bulk liquid approximately follows the Stokes-Einstein relation $D = k_B T/6\pi\eta R$, where $R$ is the effective radius of the molecule and $\eta$ is the solvent's viscosity. Small ions diffuses slower than expected from this formula and furthermore their mobility increases as the ion radius increases, opposite of the Stokes-Einstein relation.[45, 52] This is because a small ion is able to hold on to its hydration shell, effectively increasing its size.

Considering next a hydronium ion whose size is approximately equal to that of $K^+$ [53], so one would expect a similar diffusion constant. This is not case: $D(K^+) = 0.196Å^2/ps$, whereas $D(H_3O^+) = 0.931$ $Å^2/ps$, both at 298K[53, 54]. The faster diffusion of the hydronium ion is attributed to the Grotthuss mechanism for proton conduction in bulk water, which involves the quantum shuttling of hydrogen atoms along hydrogen bonded water molecules[55-58]. The classical hydronium ion considered here lacks this feature, so we expect slower dynamics. Nevertheless, the calculations are still useful for additional insight into the surface effect and as a benchmark when the quantum nature of the proton is taken into account in future work.

The results of our calculations are shown in Figure 10. For normal water-DCE interactions (coupling constant $f_S = 1$), the hydronium diffusion constant decreases from 0.12 $Å^2/ps$ in bulk water (which is close to values calculated with other models of classical $H_3O^+$[59] and significantly slower than the experimental value as explained above), to near 0.07 $Å^2/ps$ when the ion is about two water diameters into the DCE phase, then increases as the ion is getting deeper into the organic phase. As $f_S$ is reduced, the decrease in $D_{||}$ as the ion begin to cross the interface is not as marked. The turnaround around $Z = 5Å$ when $D_{||}$ begins to rise again is still observed. Finally, when $f_S = 0.1$, no significant surface affect is observed.

These results are consistent with the structural data presented above. As the ion begin to cross the interface, its mobility in the direction parallel to the interface is slowed down by the fact that it is encored to a wide water cone and to a water finger as $Z$ increases. Reducing $f_S$ and thus the magnitude of the water finger, will reduce the impact of this effect on $D_{\|}$. Finally, when the finger breaks, the hydrated ion cluster is free to move in the organic phase with a diffusion constant that is larger than in bulk water due to the reduced effective dielectric friction[43, 60].

## IV. SUMMARY AND CONCLUSIONS

The transfer of the classical hydronium ion across the water/1,2-dichloroethane interface has been studied as a function of the surface tension of the neat interface by varying the interaction strength between the two liquids thus providing new insight into the structural and dynamical factors influencing ion transfer across the interface. As the interaction between the two liquids weakens, rise in interfacial tension and decrease width have major impact on the thermodynamics and dynamics of the transfer. The ion transfer involves the co-transfer of three water molecules independent of the surface tension. However, as the surface tension increases, intrinsic water fingering and capillary fluctuations decreases and fewer water molecules are co-transported with the ion in the second shell. This explains the surprising result that the net free energy of transfer moderately increases as the surface tension increases.

As found in previous studies, ion transfer is facilitated by formation of water fingers attached to the ion. Reducing the interface roughness (and correspondingly the amplitude of the intrinsic water fingers in the neat interface) leads to a reduction in the length of the finger that the ion is attached to, consistent with the reduced size of the second hydration shell.

Dynamical properties are calculated during the ion transfer process including residence time for water molecules in the first hydration shell and lateral ion diffusion constants. These varies with the surface tension in a way that are consistent with the structural insight summarized above.

## ACKNOWLEDGMENTS

Financial support from the National Science Foundation through grant CHE-1800158 is acknowledged.

## REFERENCES

1. Adamson, A. W., *Physical Chemistry of Surfaces*. Fifth ed.; Wiley: New York, 1990.

2. Rowlinson, J. S.; Widom, B., *Molecular Theory of Capillarity*. Clarendon: Oxford, 1982.

3. Benjamin, I., Molecular structure and dynamics at liquid-liquid interfaces. *Annu. Rev. Phys. Chem.* **1997,** *48*, 401.

4. Chorny, I.; Benjamin, I., Hydration shell exchange dynamics during ion transfer across the liquid/liquid interface. *J. Phys. Chem. B* **2005,** *109* (34), 16455-16462.

5. Chang, T. M.; Dang, L. X., Recent advances in molecular simulations of ion solvation at liquid interfaces. *Chem. Rev.* **2006,** *106* (4), 1305-1322.

6. Dryfe, R. A. W., The Electrified Liquid-Liquid Interface. *Adv. Chem. Phys.* **2009,** *141*, 153-215.

7. Kikkawa, N.; Wang, L. J.; Morita, A., Microscopic Barrier Mechanism of Ion Transport through Liquid-Liquid Interface. *J. Am. Chem. Soc.* **2015,** *137* (25), 8022-8025.

8. Benjamin, I., Reactivity and Dynamics at Liquid Interfaces. *Rev. Comput. Chem.* **2015,** *28*, 205-313.

9. Karnes, J. J.; Benjamin, I., Geometric and energetic considerations of surface fluctuations during ion transfer across the water-immiscible organic liquid interface. *J. Chem. Phys.* **2016,** *145* (1).

10. Benjamin, I., Hydronium ion at the water/1,2-dichloroethane interface: Structure, thermodynamics, and dynamics of ion transfer. *J. Chem. Phys.* **2019,** *151* (9).

11. Kumar, N.; Servis, M.; Liu, Z.; Clark, A. E., Competitive Interactions at Electrolyte/Octanol Interfaces: A Molecular Perspective. *J. Phys. Chem. C* **2020,** *124* (20), 10924-10934.

12. Marcus, R. A., On the theory of ion transfer rates across the interface of two immiscible liquids. *J. Chem. Phys.* **2000,** *113*, 1618-1629.

13. Kornyshev, A. A.; Kuznetsov, A. M.; Urbach, M., Coupled ion-interface dynamics and ion transfer across the interface of two immiscible liquids. *J. Chem. Phys.* **2002,** *117*, 6766-6779.

14. Verdes, C. G.; Urbakh, M.; Kornyshev, A. A., Surface tension and ion transfer across the interface of two immiscible electrolytes. *Electrochem. Commun.* **2004,** *6* (7), 693-699.

15. Jorge, M.; Cordeiro, M. N. D. S., Intrinsic Structure and Dynamics of the Water/Nitrobenzene Interface. *J. Phys. Chem. C* **2007,** *111*, 17612-17626.

16. Bresme, F.; Chacón, E.; Tarazona, P.; Tay, K., Intrinsic structure of hydrophobic surfaces: The oil-water interface. *Phys. Rev. Lett.* **2008,** *101* (5).

17. Willard, A. P.; Chandler, D., Instantaneous Liquid Interfaces. *J. Phys. Chem. B* **2010,** *114* (5), 1954-1958.

18. Jorge, M.; Hantal, G.; Jedlovszky, P.; Cordeiro, M. N. D. S., Critical Assessment of Methods for the Intrinsic Analysis of Liquid Interfaces: 2. Density Profiles. *J. Phys. Chem. C* **2010,** *114* (43), 18656-18663.

19. Kikkawa, N.; Wang, L.; Morita, A., Computational study of effect of water finger on ion transport through water-oil interface. *J. Chem. Phys.* **2016,** *145* (1), 014702.

20. Monroe, C. W.; Urbakh, M.; Kornyshev, A. A., The distinctive electrowetting properties of ITIES. *J Phys-Condens Mat* **2007,** *19* (37).

21. Schweighofer, K. J.; Benjamin, I., Electric field effects on the structure and dynamics at a liquid/liquid interface. *J. Electroanal. Chem.* **1995,** *391*, 1.

22. Kornyshev, A. A.; Kuznetsov, A. M.; Urbakh, M., Coupled ion-interface dynamics and ion transfer across the interface of two immiscible liquids. *J. Chem. Phys.* **2002,** *117* (14), 6766-6779.

23. Hill, A. W.; Benjamin, I., Influence of surface tension on adsorbate molecular rotation at liquid/liquid interfaces. *J. Phys. Chem. B* **2004,** *108* (40), 15443-15445.

24. Benay, G.; Wipff, G., Liquid-Liquid Extraction of Uranyl by TBP: The TBP and Ions Models and Related Interfacial Features Revisited by MD and PMF Simulations. *J. Phys. Chem. B* **2014,** *118* (11), 3133-3149.

25. Kuchitsu, K.; Morino, Y., Estimation of anharmonic potential constants. II. Bent XY2 molecules. *Bull. Chem. Soc. Jpn.* **1965,** *38*, 814-824.

26. Benjamin, I., Theoretical study of the water/1,2-dichloroethane interface: Structure, dynamics and conformational equilibria at the liquid-liquid interface. *J. Chem. Phys.* **1992,** *97*, 1432-1445.

27. Lee, H. S.; Tuckerman, M. E., Ab Initio Molecular Dynamics Studies of the Liquid-Vapor Interface of an HCl Solution. *J. Phys. Chem. A* **2009,** *113* (10), 2144-2151.

28. Jagoda-Cwiklik, B.; Cwiklik, L.; Jungwirth, P., Behavior of the Eigen Form of Hydronium at the Air/Water Interface. *J. Phys. Chem. A* **2011,** *115* (23), 5881-5886.

29. Dang, L. X., Solvation of the hydronium ion at the water liquid/vapor interface. *J. Chem. Phys.* **2003,** *119* (12), 6351-6353.

30. Wolf, M. G.; Groenhof, G., Explicit Proton Transfer in Classical Molecular Dynamics Simulations. *J. Comput. Chem.* **2014,** *35* (8), 657-671.

31. Wolf, M. G.; Grubmuller, H.; Groenhof, G., Anomalous Surface Diffusion of Protons on Lipid Membranes. *Biophys. J.* **2014,** *107* (1), 76-87.

32. Allen, M. P.; Tildesley, D. J., *Computer Simulation of Liquids*. Clarendon: Oxford, 1987.

33. Kumar, S.; Rosenberg, J. M.; Bouzida, D.; Swendsen, R. H.; Kollman, P. A., Multidimensional Free-Energy Calculations Using the Weighted Histogram Analysis Method. *J. Comput. Chem.* **1995,** *16* (11), 1339-1350.

34. Kastner, J., Umbrella sampling. *Wires Comput Mol Sci* **2011,** *1* (6), 932-942.

35. Benjamin, I., Mechanism and dynamics of ion transfer across a liquid-liquid interface. *Science* **1993,** *261*, 1558-1560.

36. Wick, C. D.; Dang, L. X., Molecular dynamics study of ion transfer and distribution at the interface of water and 1,2-dichlorethane. *J. Phys. Chem. C* **2008,** *112* (3), 647-649.

37. Qiao, B. F.; Muntean, J. V.; de la Cruz, M. O.; Ellis, R. J., Ion Transport Mechanisms in Liquid-Liquid Interface. *Langmuir* **2017,** *33* (24), 6135-6142.

38. Karnes, J. J.; Villavicencio, N.; Benjamin, I., Transfer of an erbium ion across the water/dodecane interface: Structure and thermodynamics via molecular dynamics simulations. *Chemical Physics Letters* **2019,** *737*.

39. Berendsen, H. J. C.; Grigera, J. R.; Straatsma, T. P., The Missing Term in Effective Pair Potentials. *J Phys Chem-Us* **1987,** *91* (24), 6269-6271.

40. Koneshan, S.; Rasaiah, J. C.; Lynden-Bell, R. M.; Lee, S. H., Solvent Structure, Dynamics, and Ion Mobility in Aqueous Solutions at 25 °C. *J. Phys. Chem. B* **1998,** *102*, 4193-4204.

41. Laage, D.; Hynes, J. T., On the Residence Time for Water in a Solute Hydration Shell: Application to Aqueous Halide Solutions. *J. Phys. Chem. B.* **2008,** *112*, 7697-7701.

42. Lee, S. H.; Rasaiah, J. C., Molecular dynamics simulation of ionic mobility. 2. Alkali metal and Halide ions using the SPC/E model for water at 25 [degree] C. *J. Phys. Chem.* **1996,** *100*, 1420-1425.

43. Benjamin, I., Structure and dynamics of hydrated ions in a water-immiscible organic solvent. *J. Phys. Chem. B* **2008,** *112*, 15801-15806.

44. Benjamin, I., Molecular dynamics study of hydrated alkali and halide ions in liquid nitrobenze. *J. Electroanal. Chem.* **2010,** *650*, 41-46.

45. Impey, R. W.; Madden, P. A.; McDonald, I. R., Hydration and mobility of ions in solution. *J. Phys. Chem.* **1983,** *87*, 5071.

46. Lee, S. H.; Rossky, P. J., A comparison of the structure and dynamics of liquid water at hydrophobic and hydrophilic surfaces - a molecular-dynamics simulation study. *J. Chem. Phys.* **1994,** *100* (4), 3334-3345.

47. Bizzarri, A. R.; Cannistraro, S., Molecular Dynamics of Water at the Protein-Solvent Interface. *J. Phys. Chem. B,* **2002,** *106*, 6617 -6633.

48. Roy, S.; Dang, L. X., Water exchange dynamics around H3O+ and OH- ions. *Chem Phys Lett* **2015,** *628*, 30-34.

49. Chandler, D., *Introduction to Modern Statistical Mechanics*. Oxford University Press: Oxford, 1987.

50. Liu, P.; Harder, E.; Berne, B. J., On the calculation of diffusion coefficients in confined fluids and interfaces with an application to the liquid-vapor interface of water. *J. Phys. Chem. B* **2004,** *108* (21), 6595-6602.

51. Duque, D.; Tarazona, P.; Chacón, E., Diffusion at the liquid-vapor interface. *J. Chem. Phys.* **2008,** *128* (13), 134704

52. Robinson, R. A.; Stokes, R. H., *Electrolyte Solutions*. Butterworths: London, 1955.

53. Marcus, Y., *Ions In Solution And Their Solvation*. Wiley: Hoboken, New Jersey, 2015.

54. Light, T. S.; Licht, S.; Bevilacqua, A. C.; Morash, K. R., The fundamental conductivity and resistivity of water. *Electrochem. Solid State Lett.* **2005,** *8* (1), E16-E19.

55. Chen, H. N.; Voth, G. A.; Agmon, N., Kinetics of Proton Migration in Liquid Water. *J. Phys. Chem. B* **2010,** *114* (1), 333-339.

56. Peng, Y. X.; Swanson, J. M. J.; Kang, S. G.; Zhou, R. H.; Voth, G. A., Hydrated Excess Protons Can Create Their Own Water Wires. *J Phys Chem B* **2015,** *119* (29), 9212-9218.

57. Knight, C.; Voth, G. A., The Curious Case of the Hydrated Proton. *Acc. Chem. Res.* **2012,** *45* (1), 101-109.

58. Hassanali, A.; Giberti, F.; Cuny, J.; Kuhne, T. D.; Parrinello, M., Proton transfer through the water gossamer. *Proc. Nat. Acad. Sci. USA* **2013,** *110* (34), 13723-13728.

59. Iuchi, S.; Chen, H. N.; Paesani, F.; Voth, G. A., Hydrated Excess Proton at Water-Hydrophobic Interfaces. *J. Phys. Chem. B* **2009,** *113* (13), 4017-4030.

60. Wolynes, P. G., Dynamics of electrolyte solutions. *Annu. Rev. Phys. Chem.* **1980,** *31*, 345.

TOC Graphics: